PROCEEDINGS OF SCIENCE

Resummed BK evolution with DGLAP and kinematic constraint

Krzysztof Kutak,[a] **Wanchen Li,**[b,*] **Anna Stasto**[c] **and Robert Straka**[d]

[a] *Institute of Nuclear Physics, Polish Academy of Sciences, ul. Radzikowskiego 152, 31-342, Kraków, Poland*

[b] *Department of Physics and Center for Field Theory and Particle Physics, Fudan University, Shanghai 200438, China*

[c] *Department of Physics, Penn State University, University Park, PA 16802, U.S.A.*

[d] *AGH University of Science and Technology, Krakow, Poland*

E-mail: wanchen1995@outlook.com

I presented the analysis of the small x non-linear evolution equation formulated in momentum space supplemented by higher order terms, based on our publication Phys.Rev.D 111 (2025) 11, 116021 [1]. The resummed Balitsky-Kovchegov (BK) equation is solved in a wide range of transverse momentum and longitudinal momentum fractions, extending previous studies performed in Eur. Phys. J. C 29, 521 (2003) [2] and Eur. Phys. J. C 41, 343 (2005) [3]. The linear part of the equation is motivated by the renormalization group improved small x resummation, which includes collinear splitting functions and kinematical constraints. By solving the unintegrated gluon density from the equation, we perform fits to deep inelastic scattering reduced cross section data.

QCD at the Extremes (QCDEX2025)
1–5 Sept 2025
Online

*Speaker

 ISSN 1824-8039 . Published by SISSA Medialab.

PoS(QCDEX2025)024

1. Introduction

This contribution summarizes the work presented in my talk, which is based on the analysis of the unintegrated gluon density obtained from the Balitsky–Kovchegov (BK) equation [4–6] formulated in the momentum space. The BK equation governs the non–linear small-x evolution of the gluon density $\mathcal{F}(x,k^2)$, incorporating both gluon emission and recombination effects. In momentum space, its leading–logarithmic (LL) form reads [2, 7]

$$\begin{aligned}\mathcal{F}(x,k^2) &= \mathcal{F}^{(0)}(x,k^2) + \\ &+ \int_x^1 \frac{dz}{z}\int dk'^2\,\overline{\alpha}_s(k^2,k'^2)\left[\frac{\mathcal{F}(\frac{x}{z},k'^2)}{|k^2-k'^2|} - \frac{k^2}{k'^2}\frac{\mathcal{F}(\frac{x}{z},k^2)}{|k^2-k'^2|} + \frac{k^2}{k'^2}\frac{\mathcal{F}(\frac{x}{z},k^2)}{\sqrt{k^4+4k'^4}}\right]+ \\ &- \frac{2\pi^2}{N_c^2R^2}\int_x^1\frac{dz}{z}\left\{\left[\int_{k^2}^\infty \frac{dl^2}{l^2}\,\overline{\alpha}_s(k^2,l^2)\mathcal{F}(\frac{x}{z},l^2)\right]^2 + \right. \\ &\left. + \mathcal{F}(\frac{x}{z},k^2)\int_{k^2}^\infty\frac{dl^2}{l^2}\,\overline{\alpha}_s^2(k^2,l^2)\ln\left(\frac{l^2}{k^2}\right)\mathcal{F}(\frac{x}{z},l^2)\right\}\,, \end{aligned} \tag{1}$$

Here $\mathcal{F}^{(0)}$ is the initial distribution, x the longitudinal momentum fraction, and k the transverse momentum of the emitted gluon. The first integral term corresponds to the angular–averaged BFKL kernel, while the last two lines represent the non–linear recombination term, proportional to $\mathcal{F}^2$, whose strength is determined by the effective transverse radius R of the target. Such form can be given either by Fourier transforming the position space BK equation to the momentum space to obtain dipole gluon density [2], or by accounting for merging of gluons via the triple Pomeron vertex [8].

2. Resummations

2.1 Higher order improvements to the BK evolution

Our resummed BK equation takes the following schematic form

$$\mathcal{F}(x,k^2) = \mathcal{F}^{(0)}(x,k^2) + \mathcal{K}_{res}\otimes\mathcal{F}(x,k^2) - \mathcal{V}\otimes\mathcal{F}^2(x,k^2)\,, \tag{2}$$

developed by [9, 10], with

$$\mathcal{K}_{res}\otimes\mathcal{F} \equiv \mathcal{K}_0^{\rm kc}(z;k,k') \overset{z,k'}{\otimes} \mathcal{F}(\frac{x}{z},k') + \mathcal{K}_0^{\rm coll}(z;k,k') \overset{z,k'}{\otimes} \mathcal{F}(\frac{x}{z},k')\,. \tag{3}$$

The first term in Eq. (3) is

$$\begin{aligned}&\mathcal{K}_0^{\rm kc}(z;k,k') \overset{z,k'}{\otimes} \mathcal{F}(\frac{x}{z},k') = \\ &\int_x^1\frac{dz}{z}\int dk'^2\,\overline{\alpha}_s(k^2,k'^2)\left[\frac{\mathcal{F}(\frac{x}{z},k'^2)}{|k^2-k'^2|}\Theta\left(\frac{k^2}{z}-k'^2\right) - \frac{k^2}{k'^2}\frac{\mathcal{F}(\frac{x}{z},k^2)}{|k^2-k'^2|} + \frac{k^2}{k'^2}\frac{\mathcal{F}(\frac{x}{z},k^2)}{\sqrt{k^4+4k'^4}}\,.\right]\end{aligned} \tag{4}$$

The kinematical constraint $\Theta\left(k^2/z - k'^2\right)$ term is implemented onto the real emissions only. The constraint can take different form and is proven to be effective on taming the strong rise given by the LO BFKL [11].

The second contribution in (3) is

$$\mathcal{K}_0^{\rm coll}(z;k,k') \overset{z,k'}{\otimes} \mathcal{F}(\frac{x}{z},k') = \int_x^1 \frac{dz}{z}\int_0^{k^2}\frac{dk'^2}{k^2}\,\bar{\alpha}_s(k^2)z\tilde{P}_{gg}(z)\mathcal{F}(\frac{x}{z},k') + \int_x^1 \frac{dz}{z}\int_{k^2}^{k^2/z}\frac{dk'^2}{k'^2}\,\bar{\alpha}_s(k'^2)z\frac{k'^2}{k^2}\tilde{P}_{gg}(z\frac{k'^2}{k^2})\mathcal{F}(\frac{x}{z},k')\,. \quad (5)$$

It is the sum of the collinear and anticollinear contributions, with $\tilde{P}_{gg}^{(0)} = P_{gg}^{(0)} - 1/z$ the non-singular part of the LO DGLAP gluon-gluon splitting function

$$P_{gg}^{(0)} = \frac{1-z}{z} + z(1-z) + \frac{z}{(1-z)_+} + \frac{1}{2C_A}\delta(1-z)\,\frac{11C_A - 4N_f T_r}{6}\,. \quad (6)$$

Here $C_A = 3, T_r = 1/2$ and N_f is number of quark flavors. One of the advantages of the momentum–space formulation is that the full collinear structure of the DGLAP splitting functions can be included explicitly in the evolution kernel. This provides a well–defined setup for phenomenological studies that aim to describe the unintegrated gluon density over a broad kinematic range, from the saturation region to the perturbative domain.

3. Fit results

In this section, we present the fit to the HERA data [12] and the corresponding unintegrated gluon density, obtained as the solution of Eq. (2). The initial condition is chosen in the form motivated by the Golec–Biernat–Wüsthoff (GBW) model,

$$\mathcal{F}^{(0)}(x,k) \;= A\,\alpha_s(k^2)(1-x)^{\alpha}x^{\beta}(k^2)^{\gamma}e^{-B^2k^2}. \quad (7)$$

The parameters are fitted to the reduced cross section σ_r, which is given by the combination of the two structure functions F_2 and F_L

$$\sigma_r(y,x,Q^2) = F_2(x,Q^2) - \frac{y^2}{1+(1-y)^2}F_L(x,Q^2). \quad (8)$$

where the inelasticity $y = Q^2/(sx)$ and $\sqrt{s}$ is the electron-proton center-of-mass energy. We perform the fits using $N_f = 4$ active flavors.

A main improvement over previous BK/BFKL analyses [2, 3, 13] is the extended transverse-momentum coverage of the unintegrated gluon density $\mathcal{F}(x,k^2)$. This allows the collinearly modeled contribution to the structure function F_2 [14] to be incorporated directly into the perturbative calculation, ensuring a consistent treatment across both low- and high-k^2 domains. Further technical details can be found in Ref. [1].

Figure 1 shows the fitted reduced cross section compared with the HERA data. Selecting all low-x points ($x < 0.013$) yields a total of 239 data points in the fit. Two fit scenarios are considered: one with $\Lambda_{\rm QCD}$ fixed at 0.289 GeV, following Ref. [13], and another where $\Lambda_{\rm QCD}$ is treated as a free

	α	β	A	B^2	γ	C	λ	R^2	$\Lambda_{\rm QCD}$
χ^2/dof = 1.6	0.80662	-0.42651	0.74038	0.64239	1.09987	0.6163	-0.02361	2.50003	0.499
χ^2/dof = 2.0	0.67356	-0.41625	0.65917	0.47992	1.05338	0.572	-0.00223	2.54913	fixed

Table 1: χ^2 and fit parameters in the fitted and fixed $\Lambda_{\rm QCD}$ scenarios respectively.

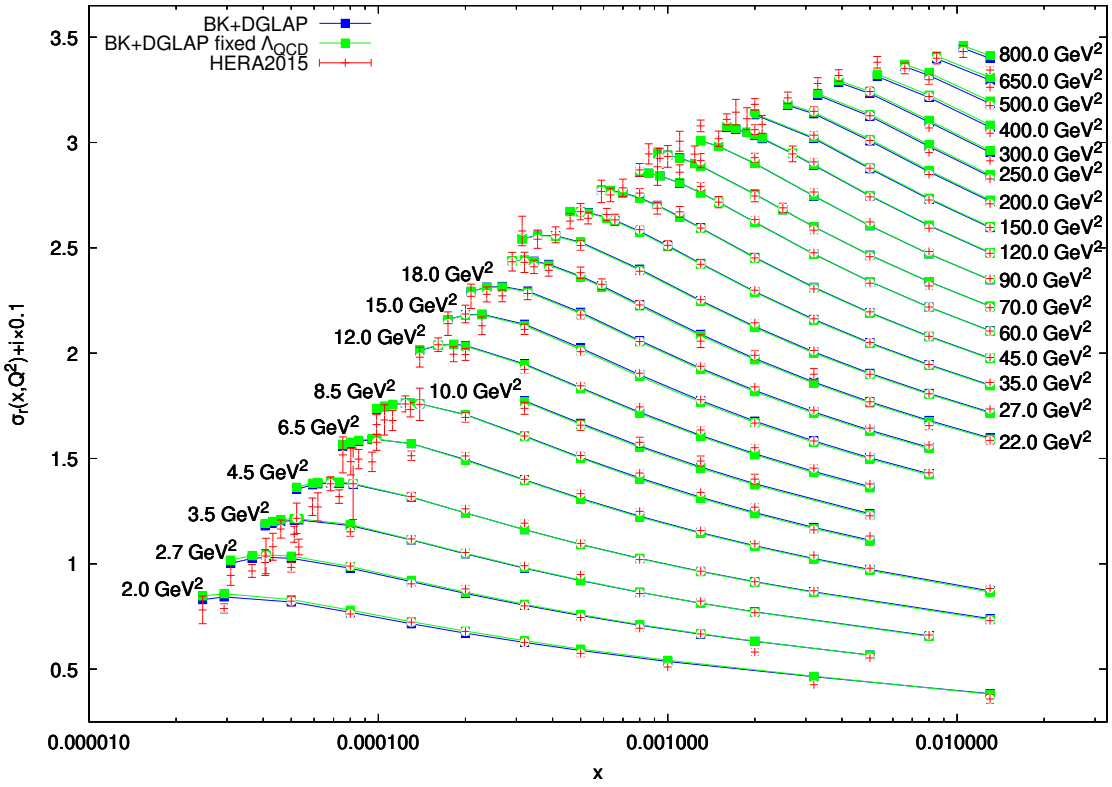

Figure 1: *Comparison between our reduced cross section fit with the HERA data. Each curve is separated with an additional offset 0.1 to better present a wider Q^2 spectrum. The blue curve is for fitted $\Lambda_{\rm QCD}$ and green curve for fixed $\Lambda_{\rm QCD}$ = 0.289 GeV.*

parameter. Both cases provide a satisfactory description of the data, with the best-fit parameters summarized in Table 1.

The resulting unintegrated gluon densities for both fits are shown in Figs. 2 and 3. Both scenarios exhibit a consistent scaling pattern of the saturation scale: as x decreases, the peak of $\mathcal{F}(x, k^2)$ shifts toward larger k^2, deeper into the perturbative region. The fitted and fixed $\Lambda_{\rm QCD}$ results are in close agreement, confirming the stability of the extracted gluon distribution.

4. Conclusions

We present an analysis of the unintegrated gluon density obtained from the momentum–space Balitsky–Kovchegov equation, incorporating resummations from the kinematical constraint and the collinear DGLAP contributions. Compared with earlier BK–based fits, the present formulation provides an improved description of data over a wide range of Q^2, yielding a consistent behavior

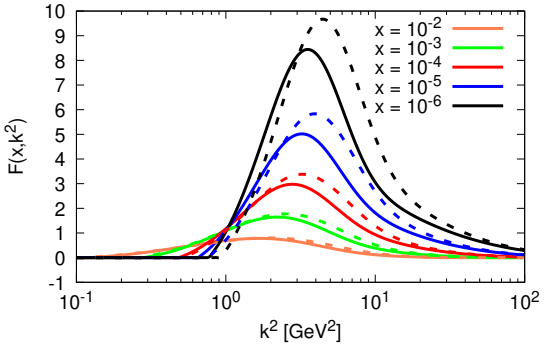

Figure 2: *Plots of fitted unintegrated gluon density as a function of k^2 for various values of x. Solid and dashed curves denote fitted and fixed $\Lambda_{\rm QCD}$.*

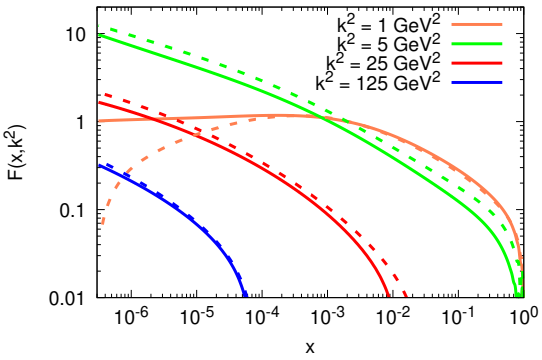

Figure 3: *Plots of fitted unintegrated gluon density as a function of x for various values of k^2. Solid and dashed curves denote fitted and fixed $\Lambda_{\rm QCD}$.*

across the full (x, k^2) spectrum of the unintegrated gluon density. The resulting gluon distribution exhibits a saturation scaling pattern consistent with previous phenomenological models and aligns with the overall QCD evolution picture.

References

[1] K. Kutak, W. Li, A. Stasto, and R. Straka, Phys. Rev. D **111**, 116021 (2025), 2502.15465.

[2] K. Kutak and J. Kwiecinski, Eur. Phys. J. C **29**, 521 (2003), hep-ph/0303209.

[3] K. Kutak and A. M. Stasto, Eur. Phys. J. C **41**, 343 (2005), hep-ph/0408117.

[4] I. Balitsky, Phys. Rev. D **60**, 014020 (1999), hep-ph/9812311.

[5] Y. V. Kovchegov, Phys. Rev. D **61**, 074018 (2000), hep-ph/9905214.

[6] Y. V. Kovchegov, Phys. Rev. D **60**, 034008 (1999), hep-ph/9901281.

[7] J. Bartels and K. Kutak, Eur. Phys. J. C **53**, 533 (2008), 0710.3060.

[8] J. Bartels and M. Wusthoff, Z. Phys. C **66**, 157 (1995).

[9] M. Ciafaloni, D. Colferai, D. Colferai, G. P. Salam, and A. M. Stasto, Phys. Lett. B **576**, 143 (2003), hep-ph/0305254.

[10] M. Ciafaloni, D. Colferai, G. P. Salam, and A. M. Stasto, Phys. Rev. D **68**, 114003 (2003), hep-ph/0307188.

[11] M. Deak, K. Kutak, W. Li, and A. M. Stasto, Eur. Phys. J. **C79**, 647 (2019), 1906.09062.

[12] H1, ZEUS, H. Abramowicz *et al.*, Eur. Phys. J. C **75**, 580 (2015), 1506.06042.

[13] W. Li and A. M. Stasto, Eur. Phys. J. C **82**, 562 (2022), 2201.10579.

[14] J. Kwiecinski, A. D. Martin, and A. M. Stasto, Phys. Rev. **D56**, 3991 (1997), hep-ph/9703445.